Ultrasound-induced Molecular Delivery to Erythrocytes using a Microfluidic System

Connor S. Centner,[1*] Emily M. Murphy,[1*] Mariah C. Priddy,[1] John T. Moore,[1] Brett R. Janis,[2] Michael A. Menze,[2] Andrew P. DeFilippis,[3] Jonathan A. Kopechek[1]

[1]Dept. of Bioengineering, University of Louisville, Louisville, KY, USA, 40292

[2]Dept. of Biology, University of Louisville, Louisville, KY, USA, 40292

[3]Dept. of Medicine, University of Medicine, Louisville, KY, USA, 40292

**authors contributed equally to this work*

Corresponding Author Information

Jonathan A. Kopechek, Ph.D.

Assistant Professor, Dept. of Bioengineering

University of Louisville

2301 S. Third St.

Lutz 419

Louisville, KY 40292

Phone: (502) 852-8205

E-mail: jonathan.kopechek@louisville.edu

Abstract

Preservation of erythrocytes in a desiccated state for storage at ambient temperature could simplify blood transfusions in austere environments such as rural clinics, far-forward military operations, and during space travel. Currently, storage of erythrocytes is limited by a short shelf-life of 42 days at 4 °C and long-term preservation requires a complex process that involves the addition and removal of glycerol from erythrocytes before and after storage at -80 °C, respectively. Natural compounds, such as trehalose, can protect cells in a desiccated state if they are present at sufficient levels inside the cell, but mammalian cell membranes lack transporters for this compound. To facilitate compound loading across the plasma membrane via ultrasound and microbubbles (sonoporation) a polydimethylsiloxane-based microfluidic device was developed. Delivery of fluorescein into erythrocytes was tested at various conditions to assess the effects of parameters such as ultrasound pressure, ultrasound pulse interval, microbubble dose, and flow rate. Changes in ultrasound pressure and mean flow rate caused statistically significant increases in fluorescein delivery of up to 73 ± 37% (p<0.05) and 44 ± 33% (p<0.01), respectively, compared to control groups, but no statistically significant differences were detected with changes in ultrasound pulse intervals. Following freeze-dying and rehydration, recovery of viable erythrocytes increased by up to 128 ± 32% after ultrasound-mediated loading of trehalose compared to control groups (p<0.05). These results suggest that ultrasound-mediated molecular delivery in microfluidic channels may be a viable approach to process erythrocytes for long-term storage in a desiccated state at ambient temperatures.

Introduction

Blood transfusions are one of the most common medical procedures performed in U.S. hospitals [1]. Current FDA-approved storage methods for erythrocytes require refrigeration at 1-6 °C for up to 42 days before blood units expire due to detrimental storage effects on morphological and biochemical properties ("storage lesions") [2-5]. The limited shelf-life of refrigerated erythrocytes can lead to shortages in supply [6, 7], especially when donations decrease due to natural disasters or other factors. Less common techniques for long-term storage include freezing at -80 °C, allowing erythrocytes to be stored for up to 10 years. However, freezing erythrocytes requires a complex and sensitive glycerol-loading process that is time-consuming and poses challenges in cases where blood transfusions are required quickly. Significant research efforts have attempted to develop artificial blood substitutes but these products have failed clinical trials [8] and no artificial blood substitutes are currently approved for routine clinical use [9]. As an alternative approach to hemoglobin-based artificial blood substitutes, recent efforts have focused on generating stem cell-derived erythrocytes [10]. These products are entering clinical trials and potentially offer a new source of erythrocytes for clinical application. However, stem cell-derived erythrocytes face similar challenges as described above — limited shelf-life and thermal stability. Alternatively, an approach to store erythrocytes in a dried state at ambient temperatures would reduce cell membrane oxidation and storage lesion, thereby increasing the shelf-life. In addition, dry preservation of erythrocytes would enable blood transfusions in locations where it is not currently feasible or extremely challenging, including remote medical centers, far forward military operations, and long-duration space missions. Therefore, there is a significant

need for an effective and inexpensive method to store erythrocytes at ambient temperatures for extended periods of time without refrigeration or freezing.

A wide variety of organisms in nature, including tardigrades ("water bears") and brine shrimp ("sea monkeys"), can survive freezing ("cryobiosis") and desiccation ("anhydrobiosis") for decades or longer before returning to normal physiological function after thawing or rehydration [11-13]. Given that entire organisms can survive desiccation it seems plausible that erythrocytes could also be preserved in this manner. The fact that erythrocytes lack nuclei and other organelles such as mitochondria would suggest that dry-preservation may be even more feasible than for more complex nucleated cells. Organisms that have developed the ability to survive desiccation generally produce various protective compounds, such as late embryogenesis abundant proteins and the non-reducing sugar trehalose, to stabilize cellular structures during the freezing and drying process. Trehalose is biocompatible and already used in vaccines and food products [14]. However, high levels of trehalose (~100 mM) are required intracellularly and mammalian cells lack transporters for this sugar. Therefore, an effective method is required to load mammalian cells with preservative compounds for desiccation [15]. Prior approaches have focused on passive loading of erythrocytes, platelets, or other mammalian cells via endocytosis, genetically engineered

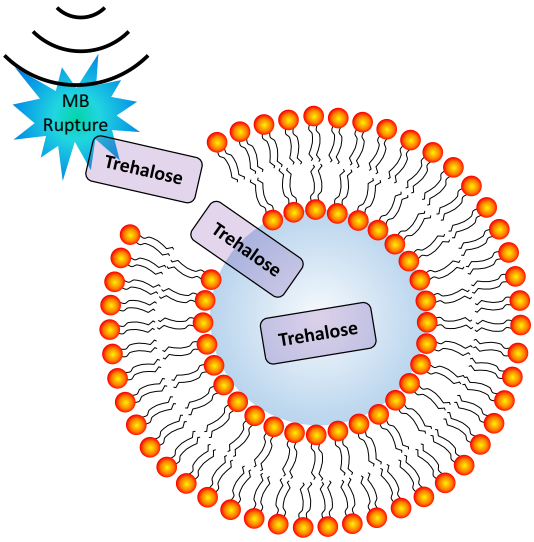

Figure 1: Illustration of ultrasound-induced microbubble (MB) rupture leading to transient perforation of cell membranes — enabling enhanced intracellular delivery of soluble compounds such as trehalose (not to scale).

pores, or electroporation [16-21]. These studies demonstrated that intracellular trehalose could protect some mammalian cells during drying and rehydration, but intracellular loading either required a long process (7+ hours) at 37 °C which increases susceptibility to oxidative damage and reduces cell viability [22] or throughput was low and inefficient. An alternative loading approach by ectopically expressing trehalose transporters in mammalian cells to facilitate uptake showed promise but scale-up of this approach to large numbers of cells is very challenging [23-25].

To address these limitations, our group is developing a novel approach to preserve erythrocytes with protective compounds such as trehalose by utilizing ultrasound and microbubbles to induce transient pore formation in cellular membranes, or “sonoporation” (Figure 1). Sonoporation can occur due to inertial cavitation when ultrasound waves at sufficient pressure amplitudes induce rapid collapse of microbubbles proximal to the cell membranes and transiently perforate the cell membrane enabling rapid uptake of molecular compounds [26]. The pores in the cell membrane typically seal quickly in an active repair process influenced by factors such as pore size and Ca^{2+} concentration [11, 27-30]. Thus, this approach can potentially enable rapid loading of compounds into cells with higher efficiency and viability compared to other methods that are solely dependent on endocytosis and/or passive diffusion [27]. Furthermore, microbubbles are approved for clinical use as intravenous ultrasound contrast agents to image cardiac blood flow [31]. Ultrasound and microbubbles are also in development for targeted gene and drug delivery applications, including delivery of trehalose into platelets [32-35].

Consistent intracellular delivery of trehalose is fundamental to preservation of cells in a desiccated state and variability in trehalose delivery may cause reduced recovery of

viable erythrocytes after drying and rehydration. To address this need for homogeneous compound delivery we have developed a microfluidic system for cell processing and molecular loading which utilizes submillimeter channels that enable consistent flow with a homogeneous mixture of erythrocytes, molecular compounds dispersed in solution, and microbubbles during ultrasound exposure. The utilization of biomicrofluidics technologies for cell processing and analysis is rapidly expanding due to the microscale manipulation capabilities. It is being studied extensively for its applications towards single-cell analysis and measurement, microscale biophysics and biochemistry manipulation, and tissue engineering. Previous studies have explored molecular delivery to cells through small microfluidic channels without ultrasound treatment [36]. The use of ultrasound-integrated biomicrofluidics ("acoustofluidics") for intracellular molecular delivery is a rapidly growing topic of interest to address current challenges in cell transfection efficiency [37, 38]. In this study we have characterized an acoustofluidic system designed to enable more consistent ultrasound and microbubble exposure of each erythrocyte compared to bulk treatment approaches, thereby leading to increased consistency of ultrasound-mediated molecular delivery.

The objective of this study was to assess the role of various ultrasound and flow parameters on the efficiency of molecular delivery into erythrocytes using an ultrasound-integrated polydimethylsiloxane (PDMS)-based microfluidic device. Although sonoporation and ultrasound-mediated molecular delivery to cells is a well-established phenomenon, this study utilizes a novel acoustofluidic setup to demonstrate the efficacy of loading erythrocytes with molecular compounds via sonoporation for dry preservation. In addition, this study yields new insights into the effects of various parameters on the

efficiency of intracellular loading in an acoustofluidic system. We assessed the delivery efficiency of a fluorescent compound (fluorescein), which can be readily detected intracellularly with flow cytometry. Various ultrasound pressures, ultrasound pulse intervals, microbubbles doses, and microfluidic flow rates were tested in order to determine the effect of each parameter. In addition, we also assessed the recovery of erythrocytes after freeze-drying and rehydration following trehalose loading with the ultrasound-integrated microfluidic system. These results aim to provide new knowledge toward optimization of ultrasound-mediated molecular delivery to cells in a microfluidic system for preservation of erythrocytes or other applications.

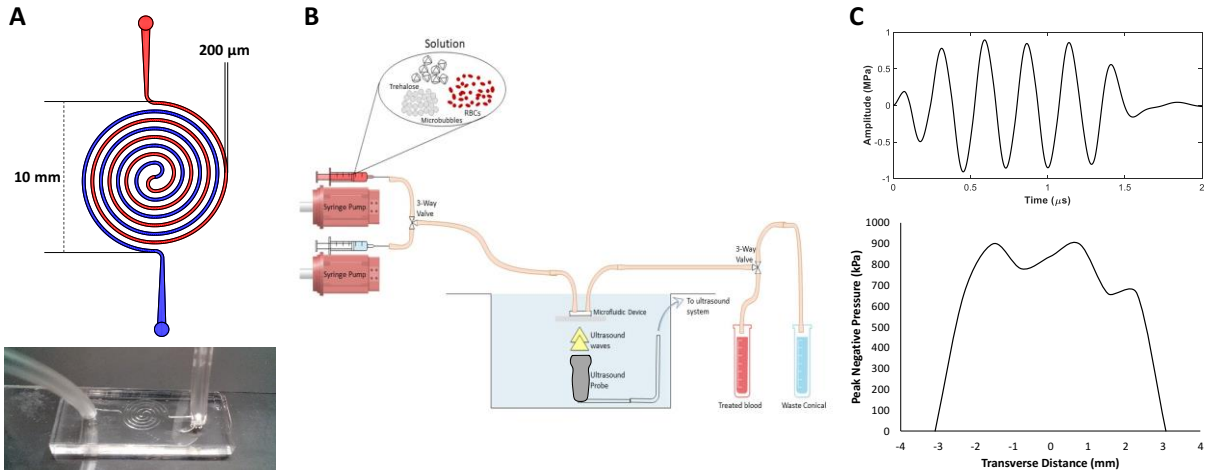

Figure 2: (A) Top: Microfluidic device design with 200 µm channel width. Bottom: a photo of one of the microfluidic devices. (B) Schematic of experimental setup (Not to scale). (C) Top: Ultrasound waveform transmitted by the ultrasound probe (ATL P4-1). Bottom: Transverse profile of the ultrasound beam (-3 dB beamwidth = ~5 mm).

Methods

Acoustofluidic device design and fabrication

Acoustofluidic devices were designed using a concentric spiral in order to maximize the time that erythrocytes were exposed to ultrasound pulses. A channel width

of 200 μm and height of 180 μm were designed to reduce shear stress on erythrocytes while increasing time spent within the ultrasound beam. Microfluidic devices were fabricated using standard photolithography techniques at the University of Louisville Micro/Nano Technology Center. A photomask was printed with a UV laser patterning system (DWL 66FS, Heidelberg Instruments, Heidelberg, Germany). SU-8 photoresist (MicroChem, Westborough, MA, USA) was spin-coated at a thickness of 200 μm on a 4" silicon wafer and cross-linked using a mask aligner (MA6/BA6, Suss, Garching, Germany) to form the master, followed by silane treatment. PDMS was obtained from Ellsworth Adhesives (Sylgard 184 Silicone Elastomer Kit, Germantown, WI, USA). A 10:1 mixture of base to curing agent was combined until a net weight of 66 grams was reached. Air bubbles were removed by vacuum for 30 min and the PDMS was pored over the SU-8 master in a 150 mm petri dish. The PDMS was cured for 2 h at 60 °C. Input and output ports were cut in the PDMS using a 2.5 mm biopsy puncher (Harris Uni-Core) and the PDMS devices were immediately bonded onto glass microscope slides after oxygen plasma treatment (100V for 60s, 500 mbar O_2, Axic HF-8 plasma asher, Gardnerville, NV, USA). To set up the microfluidic device for experiments, the device was held with clamps and ring stands at the surface of a water-filled 20-gallon aquarium tank. A segment of Tygon PVC clear tubing (1/16" ID, 1/8" OD, McMaster-Carr, Aurora, OH, USA) was inserted into the inlet and outlet ports of the device. The inlet tubing was connected to a 3-way valve. One valve was connected to a syringe filled with the erythrocyte solution on a syringe pump (NE-300, Farmingdale, NY, USA). The other valve was connected to a phosphate buffered saline (PBS) solution on a separate syringe pump to push any remaining erythrocyte sample through the tubing. The outlet tubing was connected to

another 3-way valve to allow sample collection and waste collection into 15-mL centrifuge tubes (Figure 2).

Microbubble synthesis

Ultrasound-responsive gas-filled microbubbles were synthesized to enhance intracellular delivery of molecular compounds to erythrocytes. Microbubbles were composed of a perfluorocarbon gas core encapsulated by a phospholipid shell as previously described [39]. Chloroform solutions of 1,2-distearoyl-sn-glycero-3-phosphocholine (DSPC, Avanti Lipids, Alabaster, AL, USA); 1,2-distearoyl-sn-glycero-3-ethylphosphocholine (DSEPC, Avanti Lipids); 1,2-distearoyl-sn-glycero-3-phosphoglycerol (DSPG, Avanti Lipids); and polyethylene glycol-40 stearate (Sigma-Aldrich, St. Louis, MO, USA) at the molar ratio of 100:43:1:4.5 were dried with argon gas. An aqueous micellar lipid solution was prepared by adding PBS and sonicating (Qsonica, Newtown, CT, USA) to disperse the lipids. The resulting 10 mg/mL lipid solution was diluted 1:4 in PBS and sealed in a glass vial. The vial head space was filled with decafluorobutane gas (FlouroMed, Round Rock, TX, USA), followed by amalgamation for 30 s at 4350 cpm (DB-338, COXO, Foshan City, China) to form perfluorobutane gas-filled microbubbles (MBs). This process yields microbubbles with a mean diameter of 2 ± 1 μm as previously described [34, 40].

Fluorescein delivery to erythrocytes

Human erythrocytes were obtained from de-identified clinical blood samples following protocols approved by the Institutional Review Board and stored in citrate-

phosphate-dextrose (CPD) solution with additive solution 1 (AS-1) at 4 ˚C for up to 35 days after collection [41]. A P4-1 ultrasound transducer with 96 elements (ATL, Bothell, WA, USA) on an ultrasound imaging system (Vantage 64LE, Verasonics, Kirkland, WA, USA) was placed inside the water tank below the microfluidic device and the ultrasound focus was aligned to the center of the microfluidic device at a distance of 40 mm. Ultrasound pulses were transmitted in flash mode by triggering all 96 elements of the ultrasound transducer array at the same time.

The stock erythrocyte solution was diluted with PBS to 5 million cells/mL in presence of 100 μg/mL fluorescein. Microbubbles were added shortly before running each sample through the acoustofluidic device. After treatment each sample was washed 3X via centrifugation with 1 mL of PBS to remove extracellular fluorescein prior to flow cytometry. Samples were stored on ice prior to analysis.

Flow cytometry was performed using a MACSQuant Analyzer 10 (Miltenyi Biotec, Auburn, CA, USA) with 10,000 events recorded per sample. Data were analyzed using FlowJo (Ashland, OR, USA). The mean fluorescence in the FITC channel was calculated after gating the populations on forward and side scatter plots. In addition, fluorescence microscopy images of erythrocytes were acquired with a 40X objective on an EVOS cell imaging system (American Microscopy Group, Mill Creek, Washington, USA).

Ultrasound image analysis of microbubble destruction

Ultrasound imaging was used to assess the rate of microbubble destruction at different ultrasound pressures. Microbubbles were imaged using B-mode ultrasound with a Verasonics Vantage system (ATL P4-1 probe, 2.5 MHz center frequency). A region of

interest (ROI) was selected and the mean grayscale intensity was computed using MATLAB to determine the change in contrast over time due to loss of echogenicity/microbubble destruction at different ultrasound pressures (0.5 – 1.3 MPa).

Recovery and viability of erythrocytes after freeze-drying and rehydration

The stock cell solution was diluted 40X in PBS with trehalose dissolved at a concentration of 200 mM. Microbubbles (2 %v/v) were added shortly before running the sample through the microfluidic device. After trehalose loading in the device, the samples were transferred to cryovials and frozen to -80 °C at a rate of -1 °C/min using a CoolCell container (Biocision, San Rafael, CA, USA). After storage for a minimum of 24 h at -80 °C, samples were quickly transferred to a lyophilizer (BenchTop 4K, VirTis, Los Angeles, CA, USA) and placed under vacuum below 300 mTorr for at least 48 h. After freeze-drying, samples were stored at room temperature for 24 h and rehydrated with 0.5 mL of deionized water. Recovery of erythrocytes after rehydration was determined by counting cells on a hemocytometer. Esterase activity was used as a proximate for erythrocyte viability and determined via flow cytometry using a calcein-AM (Sigma-Aldrich) viability assay.

Statistical analysis

Statistical analysis was conducted using Minitab 19 (State College, PA, USA). Statistical comparisons between groups were determined using ANOVA with statistical significance defined as $p<0.05$ (two-tailed). Post-hoc analysis was performed using Tukey's test for one-way ANOVA. Bars represent mean ± standard deviations.

Results

Effect of ultrasound and flow parameters on erythrocyte viability

Viability of erythrocytes was assessed using flow cytometry after treatment with various ultrasound and flow parameters (Figure 3). A representative flow cytometry scatter plot is shown in Figure 3A indicating the gating used to determine erythrocyte viability. There was high viability in all groups (>80%) with no statistically significant differences between different ultrasound pressures or different pulse intervals. A statistically significant decrease in viability was observed at the highest microbubble dose tested (9% v/v, ANOVA $p < 0.05$) and also at a microfluidic flow rate of 20 mL/h ($p < 0.05$), but viability remained above 80% in those groups.

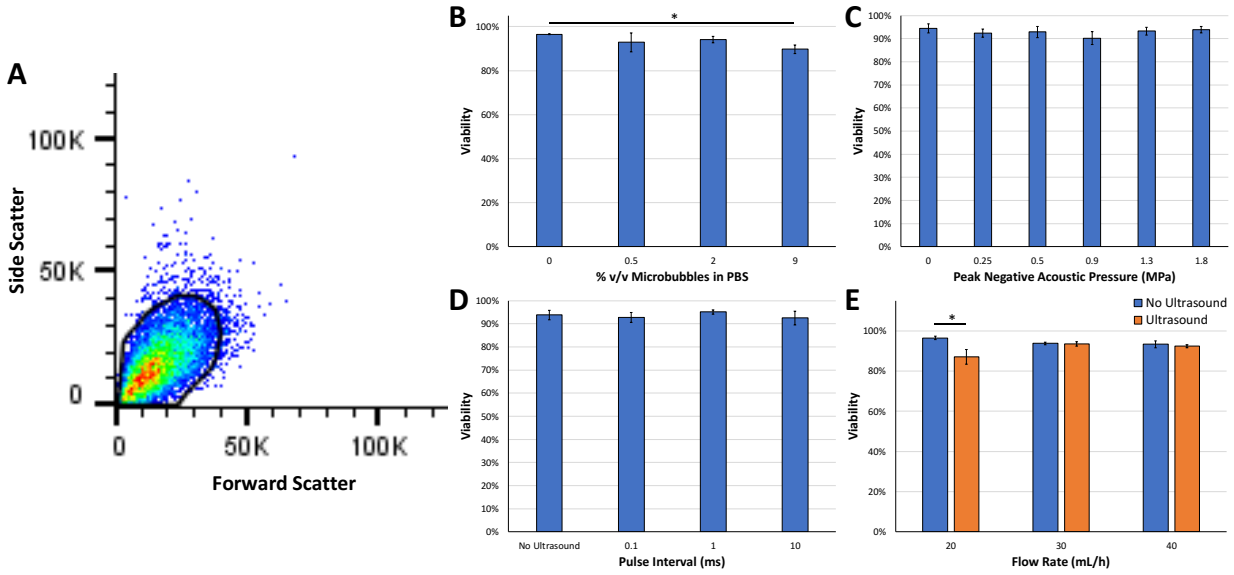

Figure 3: (A) Representative flow cytometry scatter plot with the gate used to detect viable erythrocytes based on forward and side scatter profiles. High viability of erythrocytes was observed at (B) different microbubble concentrations, (C) different acoustic pressures, (D) different pulse intervals, and (E) different microfluidic flow rates. Statistically significant decreases in viability were detected at a microbubble dose of 9% (ANOVA $p < 0.05$) and with ultrasound treatment at a microfluidic flow rate of 20 mL/h ($p < 0.05$) compared to the no ultrasound control groups.

Effect of ultrasound and flow parameters on fluorescein delivery into erythrocytes

Ultrasound-mediated intracellular delivery of fluorescein to erythrocytes was evaluated at various microbubble concentrations in PBS (%v/v) as measured by flow cytometry post-treatment. There was a trend toward a statistically significant difference in fluorescein uptake at a microbubble dose of 2% compared to the control group which passed through the microfluidic device without ultrasound or microbubbles (Figure 4A, n=4, ANOVA p=0.12).

Intracellular delivery of fluorescein to erythrocytes at varying ultrasound pressures was assessed by flow cytometry. Since a microbubble dose of 2 %v/v yielded the highest amount of fluorescein delivery as shown in Figure 4, the effect of peak negative pressure on loading efficiency was examined at this concentration. Ultrasound treatment enhanced intracellular delivery by up to 73 ± 37% compared to no ultrasound (ANOVA p<0.05). Tukey's test indicated statistically significant differences in intracellular delivery between the control group (0 MPa) and ultrasound pressures of 0.5 MPa or 0.9 MPa (Figure 4B).

The impact of pulse intervals on compound delivery was investigated and ultrasound-mediated intracellular delivery of fluorescein was assessed at pulse intervals ranging from 0.1-10 ms. No statistical differences in fluorescein delivery, as measured by flow cytometry, were detected between different pulse intervals (Figure 4C, p>0.05, n=3-4/group).

Another factor that can impact the efficiency of ultrasound-mediated molecular delivery is the time that cells are exposed to ultrasound waves, which directly correlates with the flow rate through the microfluidic device. Therefore, ultrasound-mediated intracellular delivery of fluorescein was examined at varying mean flow rates with or

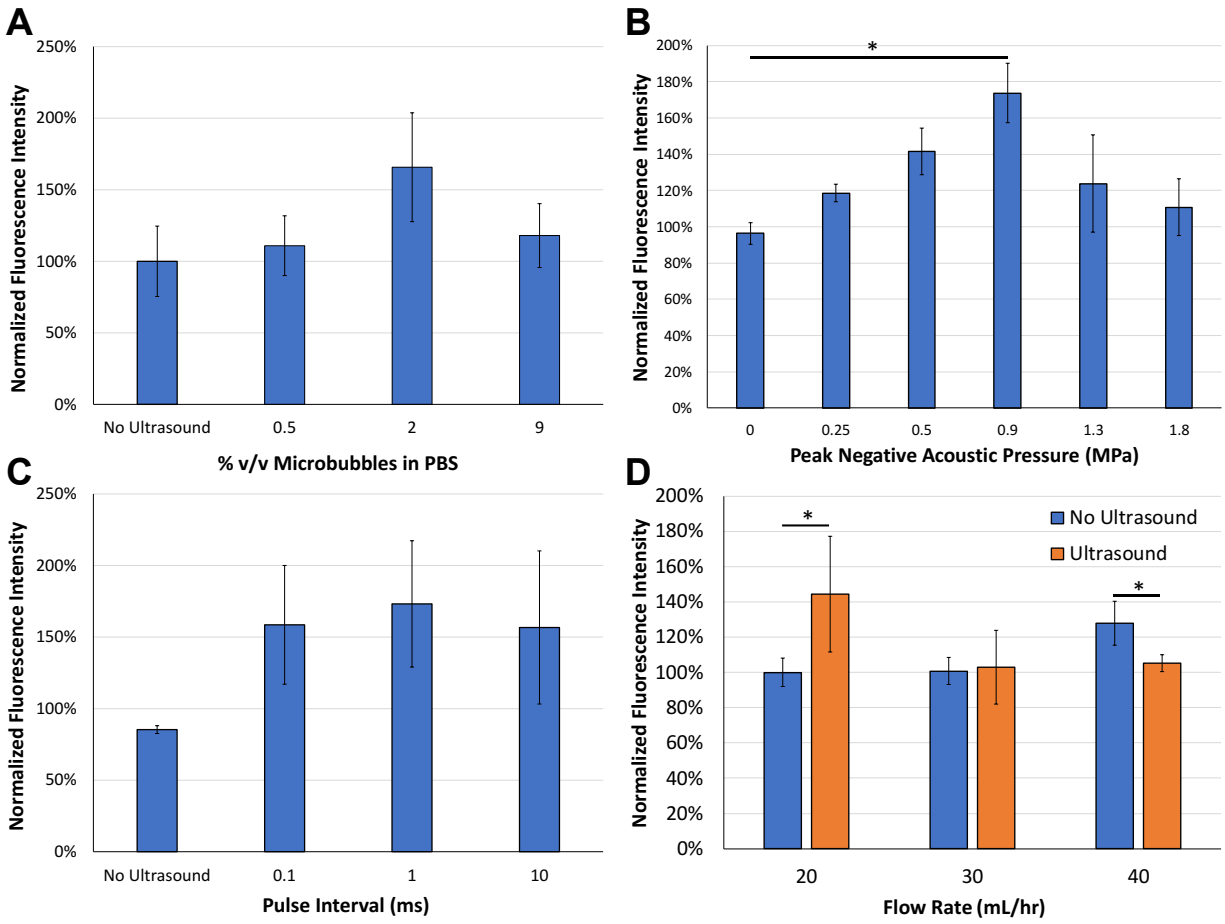

Figure 4: (A) Effect of microbubble concentrations on ultrasound-mediated fluorescein uptake. There was a trend toward statistical significance (ANOVA p=0.12, n=4/group). (B) Effect of peak negative acoustic pressure on ultrasound-mediated fluorescein uptake. There were statistically significant differences with ultrasound pressures at 0.5 and 0.9 MPa compared to the 0 MPa (no ultrasound) control group (ANOVA p = 0.01, n=4-7/group). (C) Effect of pulse interval on ultrasound-mediated fluorescein uptake. There were no statistically significant differences between the different pulse intervals (n=4-5/group). (D) Effect of microfluidic flow rate on ultrasound-mediated fluorescein uptake. Ultrasound treatment and flow rate effect fluorescein uptake, respectively (p < 0.05, n=5/group).

without ultrasound treatment. No statistically significant differences in fluorescein delivery were observed at different flow rates without ultrasound. On the other hand, ultrasound treatment enhanced intracellular delivery of fluorescein by up to 44 ± 33% to erythrocytes at mean flow rates of 20 mL/hr and 30 mL/hr compared to no ultrasound groups, but not at a higher mean flow rate of 40 mL/hr (Figure 4D, p< 0.05, n=5/group). In addition,

ultrasound treatment at a microfluidic flow rate of 20 mL/hr enhanced fluorescein delivery by 40 ± 32% compared to ultrasound treatment at a flow rate of 30 mL/hr.

Representative flow cytometry histograms are shown in Figure 5A which demonstrate the increase in fluorescence intensity of erythrocytes after fluorescein delivery at ultrasound pressures up to 0.9 MPa. In addition, a representative fluorescence microscopy image demonstrates enhanced fluorescence of the erythrocyte after ultrasound-mediated loading with fluorescein (Figure 5B). The fluorescence intensity of erythrocytes increased slightly 30 minutes and remained relatively constant up to 60 minutes after treatment, suggesting that leakage was minimal in that time frame (Figure 5C).

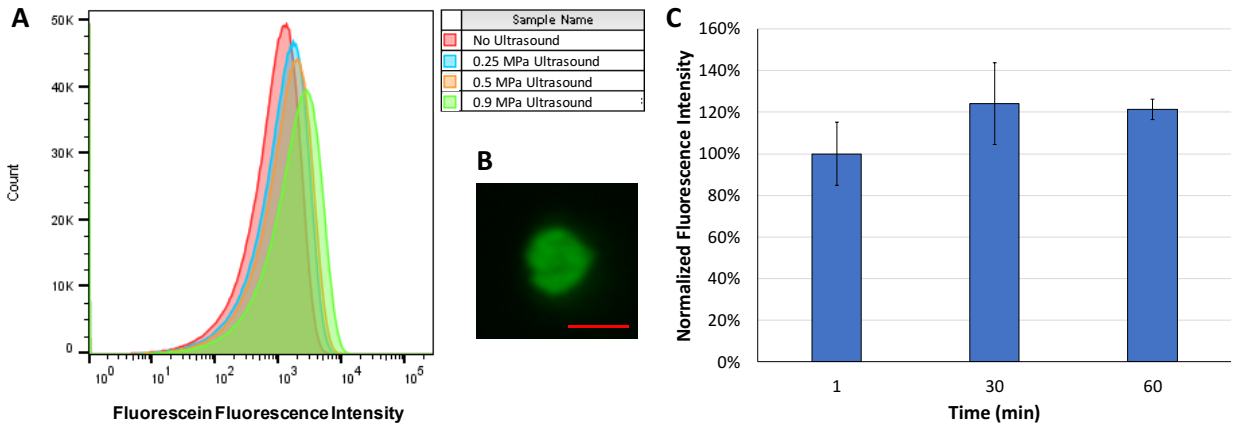

Figure 5: (A) Representative fluorescence intensity histograms after ultrasound treatment at peak negative pressures of 0.25 MPa, 0.5 MPa, 0.9 MPa, or no ultrasound (negative control). Fluorescence intensity increased up to peak negative acoustic pressures of 0.9 MPa indicating enhance molecular delivery to erythrocytes. (B) Representative fluorescence microscopy image of an erythrocyte after ultrasound treatment at a peak negative acoustic pressure of 0.9 MPa demonstrating fluorescein delivery (scale bar = 5 μm). (C) Fluorescence intensity of erythrocytes over time after fluorescein treatment as measured by flow cytometry, indicating no significant difference over time (n=3/group).

Ultrasound Image Analysis of Microbubble Destruction

Ultrasound contrast images were acquired and analyzed to assess the effect of ultrasound pressure on microbubble destruction (Figure 6). At lower acoustic pressures (0.5 MPa and 0.9 MPa) there was only a small decrease in contrast (less than 10%) after 30 seconds of ultrasound exposure, indicating minimal microbubble destruction. However, at a higher ultrasound pressure (1.3 MPa) ultrasound image contrast decreased rapidly by over 25% within 30 seconds of ultrasound exposure, indicating a higher rate of microbubble destruction. These results suggest that there is a pressure threshold between 0.9 MPa and 1.3 MPa at which there is a notable increase in the rate of microbubble destruction and this could potentially have effects on the efficiency of molecular delivery at different acoustic pressures.

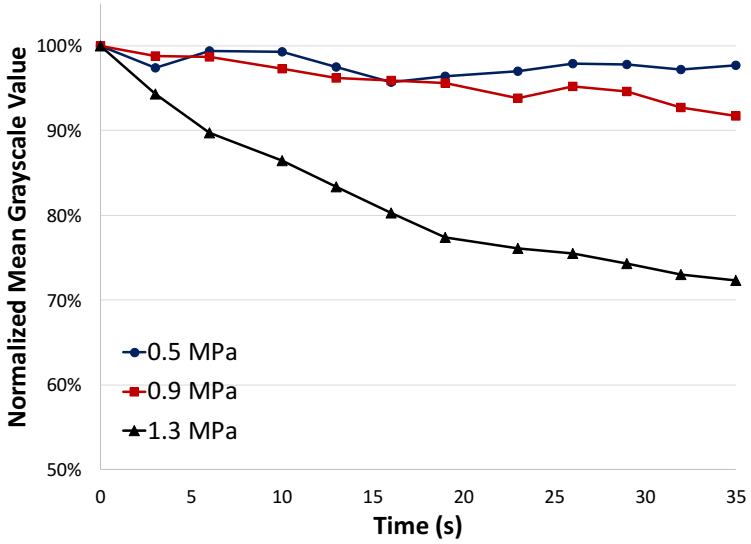

Figure 6: Ultrasound image mean grayscale intensity as a function of time at peak negative acoustic pressures of 0.5 MPa, 0.9 MPa, and 1.3 MPa. At higher pressures (1.3 MPa), the mean grayscale value decreases more rapidly indicating higher rates of microbubble destruction compared to lower pressures (0.5 MPa and 0.9 MPa).

Recovery and viability of erythrocytes after freeze-drying and rehydration

Recovery of intact viable erythrocytes was assessed across multiple conditions after freeze-drying and rehydration. Recovery of viable erythrocytes increased by up to 128 ± 32% when trehalose and microbubbles were loaded in PBS solution and ultrasound was applied to induce sonoporation prior to freeze-drying and rehydration, compared samples with no trehalose and/or no ultrasound treatment (Figure 7, $p<0.05$, n=4-8/group).

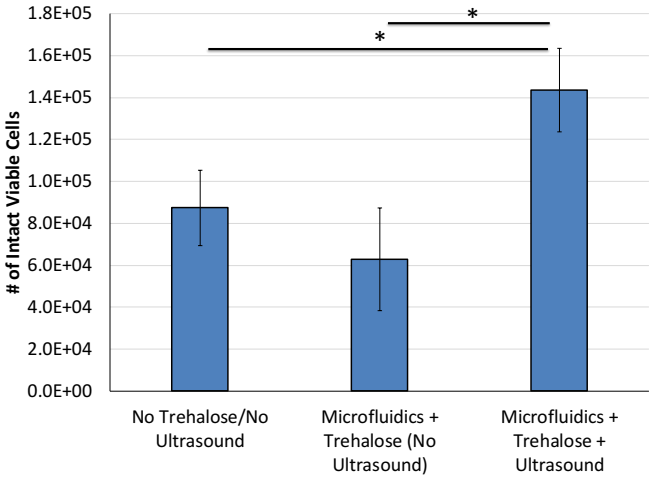

Figure 7: Number of intact viable erythrocytes following freeze-drying and rehydration. Microfluidic ultrasound treatment with trehalose caused a statistically significant increase in recovery of intact viable cells compared to the control groups ($p<0.05$, n=4-8/group).

Discussion

The development of acoustofluidics technologies is rapidly growing for a wide variety of applications [37, 42-45]. In this study, acoustofluidic devices were designed to enhance ultrasound-mediated molecular delivery to human erythrocytes. An ultrasound transducer array was used with the PDMS-based microfluidic device placed at the focal distance in order to expose cells to a relatively uniform ultrasound beam and induce transient sonoporation for rapid molecular delivery. In addition, a concentric spiral design was used for the microfluidic channels in order to maximize the time that erythrocytes were exposed to ultrasound waves as the cells passed through the channels. Using this acoustofluidic system, ultrasound-mediated intracellular delivery can be achieved in small samples

within minutes. Larger volumes can also be processed rapidly by parallelizing the acoustofluidic systems.

The results of this study demonstrate for the first time that ultrasound and microbubbles enhance molecular delivery to erythrocytes in a microfluidic device when the ultrasound pressure and microfluidic flow rate are optimized. These findings represent an early step toward development of optimized methods to produce dried blood for long-term storage at ambient temperatures. The experimental findings in this study demonstrate that several key parameters in the ultrasonic flow system have significant effects on the efficiency of intracellular molecular delivery using an acoustofluidic approach, including acoustic pressure and microfluidic flow rate. At the same time, viability remained high (>80%) for all parameters tested in this study. We conducted initial studies with fluorescein, which has a similar molecular weight as trehalose (332 Da for fluorescein and 342 Da for trehalose). Fluorescein was tested due to its fluorescent properties that enable precise intracellular detection via flow cytometry.

In this study, there was a trend toward a statistically significant difference between microbubble doses (Figure 4A), with the highest fluorescein uptake detected at a microbubble dose of 2% v/v. Lower microbubbles doses will cause lower levels of sonoporation resulting in reduced intracellular delivery, while higher microbubble doses can cause “shadowing” effects due to scattering and attenuation of ultrasound waves, resulting in reduced ultrasound pressures within part of the sample which also limits intracellular delivery. Thus, there is an optimal “therapeutic window” for the range of microbubble doses which enhance intracellular molecular delivery to cells.

The effects of ultrasound pressure and pulse interval on intracellular delivery of molecular compounds have been described in previous studies using a bulk treatment approach, but acoustofluidic-mediated molecular delivery to erythrocytes has not been previously investigated [39, 46]. In this study, a statistically significant increase in fluorescence was observed at peak negative pressures of 0.5 MPa and 0.9 MPa compared to the no ultrasound control group (Figure 4B and Figure 5). These results indicate that 0.5 MPa and 0.9 MPa induced significant sonoporation and enhanced intracellular delivery of fluorescein as erythrocytes passed through the acoustofluidic channels. Interestingly, higher acoustic pressures (1.3 MPa and 1.8 MPa) were less effective at enhancing molecular delivery. Although this result was not initially expected, it is consistent with other previous studies which found that sustained microbubble cavitation was more effective at inducing therapeutic effects compared to rapid microbubble destruction caused by inertial cavitation [47-49]. Furthermore, analysis of ultrasound image contrast from microbubbles exposed to different ultrasound pressures suggests a possible inverse correlation between the rate of microbubble destruction and fluorescein delivery, where decreased rates of microbubble destruction at lower acoustic pressures (0.5 MPa and 0.9 MPa) were associated with higher levels of fluorescein delivery compared to higher acoustic pressures.

Additionally, the effect of ultrasound pulse interval was investigated but no statistically significant difference in fluorescence was observed between each pulse interval that was tested (Figure 4C). This suggests that differences in ultrasound pulse intervals in the range of 0.1 – 10 ms are not a significant factor in molecular delivery. However, very short pulse intervals or higher duty cycles were not tested in this study and may have a more

significant impact on molecular delivery. Other studies which used a static bulk treatment approach have reported that ultrasound duty cycle can influence the efficiency of molecular delivery to cultured cells, and it is likely that a wider range of pulse intervals and duty cycles in acoustofluidic devices would cause differences in intracellular delivery as well [50, 51].

The results of this study also indicate that the microfluidic flow rate is an important parameter that affects the efficiency of ultrasound-mediated molecular delivery to erythrocytes. Interestingly, the fluorescence intensity at 40 mL/hr was actually higher without ultrasound compared to the ultrasound treated group ($p < 0.05$). This finding was unexpected and the mechanism is not fully understood, although it is likely due to a combination of multiple separate factors. Shear forces on the cells are higher at increased flow rates, so as the flow rate increases and shear forces become more significant the permeability of the cells increases and passive fluorescein uptake is greater, even without ultrasound. When ultrasound is present the microbubbles surround the cell membrane and may potentially have a shielding effect on shear forces in the surrounding fluid. On the other hand, the high flow rates reduce the amount of time that erythrocyte are exposed to ultrasound as they flow through the channels, which also limits fluorescein uptake. These effects could potentially explain the results observed at a higher flow rate of 40 mL/hr. Relatively low flow rates were used in the concentric spiral acoustofluidic system for two reasons: (1) to increase the number of ultrasound pulses that each cell experiences as it passes through the microfluidic channels, and (2) to reduce shear stress on cells in the microfluidic channels. If the flow rate is too high some cells could pass through the microfluidic chamber between pulses. Additionally, high flow rates can

increase pressures within the channels and cause failure of the PDMS-bonded devices [52].

Freeze-drying is a low temperature dehydration process that involves the removal of ice through sublimation to allow product storage in a desiccated state. Intracellular delivery of trehalose is critical for cell preservation in a desiccated state and freeze-drying erythrocytes without trehalose or with only extracellular trehalose (without ultrasound-induced sonoporation to load trehalose intracellularly) yielded low recovery of intact, viable erythrocytes compared to acoustofluidic treatment (Figure 7). This indicates that flowing erythrocytes through the microfluidic channels alone without ultrasound exposure does not induce sufficient uptake of trehalose to confer protection during freeze-drying. However, ultrasound exposure of erythrocytes with trehalose in the microfluidic system significantly increased recovery of intact and viable erythrocytes after freeze-drying and rehydration (Figure 7). This finding suggests that optimized acoustofluidic parameters can enhance intracellular trehalose delivery which is required for successful recovery of viable erythrocytes after freeze-drying.

This study explored ultrasound-enhanced delivery of small molecules (*i.e.*, fluorescein and trehalose). Larger molecules can also be delivered intracellularly using sonoporation but the uptake efficiency is decreased as we have previously described [39]. There are two important limitations to results of this study. The recovery of erythrocytes after freeze-drying and rehydration was less than 5% even after acoustofluidic-mediated trehalose loading. Further optimization of the freezing and drying process is needed and additional improvements in acoustofluidic techniques are also possible. In addition, other trehalose concentrations can be tested to determine if a higher trehalose concentration

would increase trehalose delivery and erythrocyte recovery after freeze-drying and rehydration. The optimal trehalose concentration will be within a specific “therapeutic window.” If the extracellular trehalose concentration is too low the amount of delivery will not be sufficient to protect cells during drying and rehydration, but if the extracellular trehalose concentration is too high there would be significant osmotic stress and damage to the cells. Our study used a trehalose concentration of 200 mM based on previous studies in brine shrimp that survive drying and rehydration with trehalose at these levels [15, 53], but further optimization of the trehalose concentration may be needed for ultrasound-mediated loading. Another limitation of this study is the low erythrocyte concentration (5 million/mL), which was significantly lower than the typical concentration in whole blood (~5 billion/mL). Further studies will need to assess the feasibility of acoustofluidic molecular delivery at high concentrations. An alternative approach could involve concentrating erythrocytes via centrifugation after trehalose loading if required. Despite these limitations, the results of this study still represent important steps toward addressing the challenges of effective intracellular trehalose delivery into erythrocytes.

These results demonstrate that an acoustofluidic approach can significantly enhance intracellular molecular delivery and increase recovery of viable, intact erythrocytes after freeze-drying and rehydration. Dry storage of erythrocytes could have a fundamental impact in transfusion medicine, particularly in austere environments, air ambulance operations, remote medical centers, and long-duration space missions. Further studies will need to assess optimal microfluidic designs and other parameters (*e.g.* ultrasound frequency, cell concentration, trehalose concentration, etc.) in order to further enhance intracellular trehalose delivery to erythrocytes for dry preservation. This

acoustofluidic system is a platform technology which may also have utility for molecular delivery to other cell types such as platelets, immune cells, and stem cells. The optimal acoustofluidic parameters may be different for each cell type but it is expected that general trends will be similar and ultrasound pressure and microfluidic flow rates will be critical factors for enhanced intracellular molecular delivery.

Conclusions

The results of this study demonstrate the feasibility of an acoustofluidic approach to rapidly load human erythrocytes with molecular compounds. Key parameters that affect the efficiency of intracellular delivery include the ultrasound pressure level and the microfluidic flow rate. Acoustofluidic delivery of trehalose into erythrocytes increased the recovery of intact, viable cells after freeze-drying and rehydration. Further optimization to increase erythrocyte recovery after rehydration could eventually lead to long-term storage of blood at ambient temperatures, which would have a major impact on the feasibility of blood transfusions in austere environments such as remote medical centers, air ambulance services, far-forward military operations, and long-duration space missions.

Acknowledgements

This research was funded by the University of Louisville ExCITE program (NIH grant U01 HL127518), the NSF I-Corps program (Award #1450370), and NSF Partnership for Innovation Grant (Award #1827521). Co-authors BRJ, MAM, and JAK hold ownership in DesiCorp which may financially benefit from products related to this research.

References

1. Pfuntner, A., L.M. Wier, and C. Stocks, *Most Frequent Procedures Performed in U.S. Hospitals, 2011: Statistical Brief #165*, in *Healthcare Cost and Utilization Project (HCUP) Statistical Briefs*. 2006: Rockville (MD).
2. Haradin, A.R., R.I. Weed, and C.F. Reed, *Changes in physical properties of stored erythrocytes relationship to survival in vivo.* Transfusion, 1969. **9**(5): p. 229-37.
3. Izzo, P., et al., *Erythrocytes stored in CPD SAG-mannitol: evaluation of their deformability.* Clin Hemorheol Microcirc, 1999. **21**(3-4): p. 335-9.
4. Bunn, H.F., et al., *Hemoglobin function in stored blood.* J Clin Invest, 1969. **48**(2): p. 311-21.
5. Greenwalt, T.J., C. Zehner Sostok, and U.J. Dumaswala, *Studies in red blood cell preservation. 2. Comparison of vesicle formation, morphology, and membrane lipids during storage in AS-1 and CPDA-1.* Vox Sang, 1990. **58**(2): p. 90-3.
6. Shi, L., et al., *Blood safety and availability: continuing challenges in China's blood banking system.* Transfusion, 2014. **54**(2): p. 471-82.
7. Nightingale, S., et al., *Use of sentinel sites for daily monitoring of the US blood supply.* Transfusion, 2003. **43**(3): p. 364-72.
8. Chen, J.Y., M. Scerbo, and G. Kramer, *A review of blood substitutes: examining the history, clinical trial results, and ethics of hemoglobin-based oxygen carriers.* Clinics (Sao Paulo), 2009. **64**(8): p. 803-13.
9. Silverman, T.A. and R.B. Weiskopf, *Hemoglobin-based oxygen carriers: current status and future directions.* Transfusion, 2009. **49**(11): p. 2495-515.
10. Shah, S., X. Huang, and L. Cheng, *Concise review: stem cell-based approaches to red blood cell production for transfusion.* Stem Cells Transl Med, 2014. **3**(3): p. 346-55.
11. Crowe, J.H., et al., *Anhydrobiosis: Cellular Adaptation to Extreme Dehydration.* Handbook of Physiology, Comparative Physiology, 2011: p. 1445–1477.
12. Hengherr, S., et al., *High-temperature tolerance in anhydrobiotic tardigrades is limited by glass transition.* Physiol Biochem Zool, 2009. **82**(6): p. 749-55.
13. Tsujimoto, M., S. Imura, and H. Kanda, *Recovery and reproduction of an Antarctic tardigrade retrieved from a moss sample frozen for over 30 years.* Cryobiology, 2016. **72**(1): p. 78-81.
14. Patist, A. and H. Zoerb, *Preservation mechanisms of trehalose in food and biosystems.* Colloids Surf B Biointerfaces, 2005. **40**(2): p. 107-13.
15. Crowe, J.H., et al., *Stabilization of dry Mammalian cells: lessons from nature.* Integr Comp Biol, 2005. **45**(5): p. 810-20.
16. Arav, A. and D. Natan, *Freeze drying of red blood cells: the use of directional freezing and a new radio frequency lyophilization device.* Biopreserv Biobank, 2012. **10**(4): p. 386-94.
17. Satpathy, G.R., et al., *Loading red blood cells with trehalose: a step towards biostabilization.* Cryobiology, 2004. **49**(2): p. 123-36.
18. Zhou, X., et al., *Loading trehalose into red blood cells by electroporation and its application in freeze-drying.* Cryo Letters, 2010. **31**(2): p. 147-56.
19. Eroglu, A., et al., *Intracellular trehalose improves the survival of cryopreserved mammalian cells.* Nat Biotechnol, 2000. **18**(2): p. 163-7.

20. Shirakashi, R., et al., *Intracellular delivery of trehalose into mammalian cells by electropermeabilization.* J Membr Biol, 2002. **189**(1): p. 45-54.
21. Fitzpatrick, G.M., R. Cliff, and N. Tandon, *Thrombosomes: a platelet-derived hemostatic agent for control of noncompressible hemorrhage.* Transfusion, 2013. **53 Suppl 1**: p. 100S-106S.
22. Kanias, T. and J.P. Acker, *Trehalose loading into red blood cells is accompanied with hemoglobin oxidation and membrane lipid peroxidation.* Cryobiology, 2009. **58**(2): p. 232-9.
23. Uchida, T., et al., *Intracellular trehalose via transporter TRET1 as a method to cryoprotect CHO-K1 cells.* Cryobiology, 2017. **77**: p. 50-57.
24. Kikawada, T., et al., *Trehalose transporter 1, a facilitated and high-capacity trehalose transporter, allows exogenous trehalose uptake into cells.* Proc Natl Acad Sci U S A, 2007. **104**(28): p. 11585-90.
25. Chakraborty, N., et al., *Trehalose transporter from African chironomid larvae improves desiccation tolerance of Chinese hamster ovary cells.* Cryobiology, 2012. **64**(2): p. 91-6.
26. Fan, Z., R.E. Kumon, and C.X. Deng, *Mechanisms of microbubble-facilitated sonoporation for drug and gene delivery.* Ther Deliv, 2014. **5**(4): p. 467-86.
27. Feril, L.B., Jr., et al., *Optimized ultrasound-mediated gene transfection in cancer cells.* Cancer Sci, 2006. **97**(10): p. 1111-4.
28. Hassan, M.A., P. Campbell, and T. Kondo, *The role of Ca(2+) in ultrasound-elicited bioeffects: progress, perspectives and prospects.* Drug Discov Today, 2010. **15**(21-22): p. 892-906.
29. Kudo, N., K. Okada, and K. Yamamoto, *Sonoporation by single-shot pulsed ultrasound with microbubbles adjacent to cells.* Biophys J, 2009. **96**(12): p. 4866-76.
30. Kumon, R.E., et al., *Spatiotemporal effects of sonoporation measured by real-time calcium imaging.* Ultrasound Med Biol, 2009. **35**(3): p. 494-506.
31. Villanueva, F.S., *Myocardial perfusion imaging using ultrasound contrast agents: now or never?* JACC Cardiovasc Imaging, 2010. **3**(9): p. 944-6.
32. Hernot, S. and A.L. Klibanov, *Microbubbles in ultrasound-triggered drug and gene delivery.* Adv Drug Deliv Rev, 2008. **60**(10): p. 1153-66.
33. Zhang, S., et al., *An experimental study of the use of ultrasound to facilitate the loading of trehalose into platelets.* Cryobiology, 2009. **59**(2): p. 135-40.
34. Kopechek, J.A., et al., *Ultrasound Targeted Microbubble Destruction-Mediated Delivery of a Transcription Factor Decoy Inhibits STAT3 Signaling and Tumor Growth.* Theranostics, 2015. **5**(12): p. 1378-87.
35. Kopechek, J.A., et al., *Ultrasound and Microbubble-targeted Delivery of a microRNA Inhibitor to the Heart Suppresses Cardiac Hypertrophy and Preserves Cardiac Function.* Theranostics, 2019. **9**(23): p. 7088-7098.
36. Wang, F., et al., *Microfluidic delivery of small molecules into mammalian cells based on hydrodynamic focusing.* Biotechnol Bioeng, 2008. **100**(1): p. 150-8.
37. Bose, N., et al., *The role of acoustofluidics in targeted drug delivery.* Biomicrofluidics, 2015. **9**(5): p. 052609.
38. Carugo, D., et al., *Contrast agent-free sonoporation: The use of an ultrasonic standing wave microfluidic system for the delivery of pharmaceutical agents.* Biomicrofluidics, 2011. **5**(4): p. 44108-4410815.

39. Bhutto, D.F., et al., *Effect of Molecular Weight on Sonoporation-Mediated Uptake in Human Cells.* Ultrasound Med Biol, 2018. **44**(12): p. 2662-2672.
40. Kopechek, J.A., et al., *Cardiac Gene Expression Knockdown Using Small Inhibitory RNA-Loaded Microbubbles and Ultrasound.* PLoS One, 2016. **11**(7): p. e0159751.
41. Simon, T.L., et al., *Rossi's Principles of Transfusion Medicine*. 5 ed. 2016: John Wiley & Sons.
42. Antfolk, M., et al., *Acoustofluidic, label-free separation and simultaneous concentration of rare tumor cells from white blood cells.* Anal Chem, 2015. **87**(18): p. 9322-8.
43. Li, P. and T.J. Huang, *Applications of Acoustofluidics in Bioanalytical Chemistry.* Anal Chem, 2019. **91**(1): p. 757-767.
44. Lajoinie, G., et al., *In vitro methods to study bubble-cell interactions: Fundamentals and therapeutic applications.* Biomicrofluidics, 2016. **10**(1): p. 011501.
45. Pereno, V., et al., *Layered acoustofluidic resonators for the simultaneous optical and acoustic characterisation of cavitation dynamics, microstreaming, and biological effects.* Biomicrofluidics, 2018. **12**(3): p. 034109.
46. Sennoga, C.A., et al., *Microbubble-mediated ultrasound drug-delivery and therapeutic monitoring.* Expert Opin Drug Deliv, 2017. **14**(9): p. 1031-1043.
47. Datta, S., et al., *Correlation of cavitation with ultrasound enhancement of thrombolysis.* Ultrasound Med Biol, 2006. **32**(8): p. 1257-67.
48. Gourevich, D., et al., *In Vitro Investigation of the Individual Contributions of Ultrasound-Induced Stable and Inertial Cavitation in Targeted Drug Delivery.* Ultrasound Med Biol, 2015. **41**(7): p. 1853-64.
49. Sun, T., et al., *Closed-loop control of targeted ultrasound drug delivery across the blood-brain/tumor barriers in a rat glioma model.* Proc Natl Acad Sci U S A, 2017. **114**(48): p. E10281-E10290.
50. Rahim, A., et al., *Physical parameters affecting ultrasound/microbubble-mediated gene delivery efficiency in vitro.* Ultrasound Med Biol, 2006. **32**(8): p. 1269-79.
51. Marin, A., M. Muniruzzaman, and N. Rapoport, *Acoustic activation of drug delivery from polymeric micelles: effect of pulsed ultrasound.* J Control Release, 2001. **71**(3): p. 239-49.
52. De Cock, I., et al., *Ultrasound and microbubble mediated drug delivery: acoustic pressure as determinant for uptake via membrane pores or endocytosis.* J Control Release, 2015. **197**: p. 20-8.
53. Hand, S.C. and M.A. Menze, *Molecular approaches for improving desiccation tolerance: insights from the brine shrimp Artemia franciscana.* Planta, 2015. **242**(2): p. 379-88.